



## Fabrication of layered Al-silicate magadiites for the removal of reactive dyes from textile effluents

Khalid Ahmed<sup>a</sup>, Asif Jamal Khan<sup>b</sup>, Cleo T.G.V.M.T. Pires<sup>a</sup>, Marriam Yaminc,  
Fozia Rehman<sup>a,d,\*</sup>, Abdur Rahim<sup>a,d</sup>, Jinxi Song<sup>b</sup>, Claudio Airoidi<sup>a</sup>

<sup>a</sup>*Institute of Chemistry, University of Campinas, UNICAMP, P.O. Box 6154, 13084 -971 Campinas, SP, Brazil, emails: foziaics@yahoo.com (F. Rehman), khalid\_analyst@yahoo.com (K. Ahmed), cleo@iqm.unicamp.br (C.T.G.V.M.T. Pires), airoidi42@gmail.com (C. Airoidi)*

<sup>b</sup>*Shaanxi Key Laboratory of Earth Surface System and Environmental Carrying Capacity, College of Urban and Environmental Sciences, Northwest University, Xi'an 710127, China, emails: asifj\_khan@yahoo.com (A. J. Khan), jinxisong@nwu.edu.cn (J. Song)*

<sup>c</sup>*Laboratory of Thermodynamics of Proteins-Biochemistry-Biology, University of Campinas, UNICAMP, P.O. Box 6154, 13084 -971 Campinas, SP, Brazil, email: marriam.khalid@yahoo.com (M. Yamin)*

<sup>d</sup>*Interdisciplinary Research Centre in Biomedical Materials (IRCBM), COMSATS Institute of Information Technology, Lahore, Pakistan, email: abdurrahim@ciitlahore.edu.pk (A. Rahim)*

Received 12 July 2017; Accepted 12 December 2017

### ABSTRACT

Layered silicate magadiites were synthesized with and without structurally incorporated aluminum in the inorganic framework and characterized by nitrogen adsorption, nuclear magnetic resonance spectroscopy, thermogravimetry, X-ray diffraction and scanning electron microscopy. The modified layered alumino-silicates [Al]NaMG and [2Al]NaMG showed higher adsorption capacities for remazol yellow dye (RY), about 0.026 and 0.028 mmol g<sup>-1</sup>, respectively, when compared with the original silicate analogues (0.014 mmol g<sup>-1</sup>). Dyes adsorption isotherms are dependent on pH, contact time, concentration and adsorbent. The adsorption kinetics of RY dye was slow and the equilibrium reached in 3 to 4 h. The pH effect on adsorption process was investigated at room temperature. Kinetic data of RY adsorption onto magadiites were best fitted to pseudo-first-order kinetic model. The equilibrium data were fitted to the Langmuir, Freundlich and Sips isotherm models. The Sips model best fitted to the adsorption data. The obtained results suggest that aluminum incorporated layered silicates could be efficient and cheap materials for the removal of reactive dyes such a RY from textile effluents.

*Keywords:* Magadiite; Aluminum; Dye removal; Remazol yellow; Adsorption

### 1. Introduction

Water pollution is one of the most important global issue and is the foremost cause of diseases and deaths around the globe [1,2]. The total dye depletion is more than 10<sup>4</sup> tons/year in the textile industry worldwide, out of which about 10<sup>2</sup> tons/year of the total dye is lost during dyeing process and directly discharged into wastewater, which is a major environmental concern [3]. The untreated

textile effluents contain persistent color which is not only toxic to aquatic life through damaging and reducing the photosynthetic activity of aquatic organisms but also reduce the aesthetic nature of water [4]. Several methodologies, including physical, chemical and biological processes have been adopted to remove dyes from wastewater. Among these techniques, physical processes, including adsorption proved effective for wastewater treatment [5–7].

\* Corresponding author.

Both organic and inorganic (natural/synthetic) adsorbents were investigated for the removal of pollutants from wastewater [8–12]. Among inorganic materials layered clays have attracted great attention as they can be delaminated into unilamellar platelets exhibiting superior properties to their parent precursor [7,8]. Layered silicates have been studied for centuries and have found a wide range of applications in many fields such as catalysis [8], nanocomposites [5–8], cosmetics and pharmaceutical products [10,11], biomaterials [12] controlled drug delivery, etc. [13–15].

Layered silicate materials are well known for their remarkable adsorption and intercalation properties [7–11]. The crystal structure of layered silicates is composed of two silica tetrahedral layers at nanoscale, fused to an edge-shared octahedral sheet of either alumina or magnesia. Stacking of the layers leads to a regular van der Waals gap between the layers called the interlayer or gallery. The recrystallization of layered silicates is particularly useful for the preparation of binder less pre-shaped zeotypes, ionic exchange, lamellar swelling, etc. [9,10,12–14]. Moreover, the surface modification, particularly, with positively charged alkylammonium salts has further broadened the applications of these layered materials [9,16,17]. The layered structure, high aspect ratio and high specific surface area combined with relatively easy availability, low cost made these layered silicates being the most attractive adsorbent materials. Isomorphic substitution within the layers creates negative charges which are normally counter balanced by cations residing in the interlayer [8,15,18]. Substitution of silicon by metal ions results in change in the silicates properties. Some metal silicates were synthesized directly by the isomorphic substitution method. The advantage of this method is to acquire salt crystals with unusual morphologies, some of them showed superior access to the interior parts resulted in more efficient catalytic sites [8,9,19].

Na-magadiite ( $\text{Na}_2\text{Si}_4\text{O}_{20}\cdot 11\text{H}_2\text{O}$ ) is an alkali layered silicate with a basal spacing of 15.6 Å, composed of negatively charged layers of silicon tetrahedral with terminal oxygen atoms counter balanced by cations of hydrated sodium [20]. These charged cations allow replacement by other inorganic cations or organic cations, including cationic surfactants [21,22]. Substitution of  $\text{Si}^{4+}$  is possible through other cations and more specifically by trivalent cations such as  $\text{B}^{3+}$  or  $\text{Al}^{3+}$ . Substitution of  $\text{Si}^{4+}$  by  $\text{Al}^{3+}$  either in layered or in three-dimensional silicate frameworks results in solid acid [14,23]. The swelling character of Na-magadiite combined with high cationic exchange capacity (~220 meq/100 g magadiite) and the properties such as intercalation, ion exchange and interlamellar grafting displaced by this material have been exploited for developing new organic-inorganic composite materials [24]. The chemical modification of the stable inorganic matrix with aluminum inserted inside the layered structure allows the localized interactions and the resulting materials can be used as adsorbents [8,25], catalysts [26], molecular sieves [27] and luminescent materials [28]. Na-magadiite has been widely used as a precursor in the preparation of microporous materials such as zeolites [29].

This work deals with the synthesis of Na-magadiite and Al-magadiites using hydrothermal method. Aluminum incorporated layered silicate materials ([Al]NaMG and [2Al]

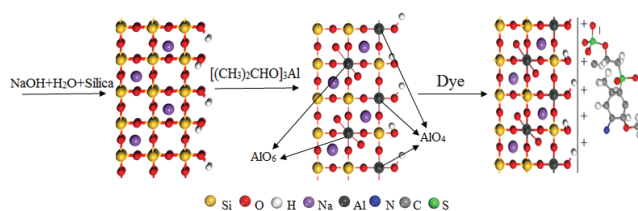


Fig. 1. Proposed synthesis of aluminum incorporated magadiite and removal of RY dye from water.

NaMG) were synthesized (Fig. 1). These materials were characterized using different techniques and applied for the removal of remazol yellow 15 dye from water. The effect of contact time and pH on adsorption process is investigated.

## 2. Materials and methods

### 2.1. Reagents

All reagents and solvents were of analytical grade purity and used as received. Silica gel, aluminum isopropoxide  $[(\text{CH}_3)_2\text{CHO}]_3\text{Al}$  (Merck, Germany), NaOH, reactive yellow 15 RY (Remazol yellow GR) (Sigma-Aldrich, Brazil) procured were used without prior purification. Deionized water was used throughout the experimentation.

### 2.2. Synthesis

Na-magadiite was synthesized using hydrothermal method with slight modification as previously reported [9]. Briefly, 3.4 g of NaOH dissolved in 76.0 g of distilled water and then 11.2 g of silica gel were added and stirred for 15 min. The resultant gel was subjected to hydrothermal treatment in an autoclave at 423 K for 18–72 h. After this treatment, the resultant solid was filtered and washed and dried at room temperature.

The aluminum incorporated magadiite derivatives [Al]NaMG and [2Al]NaMG were fabricated using the above similar procedure, with the addition of 0.46 and 0.92 g of aluminum isopropoxide  $\text{Al}[(\text{CH}_3)_2\text{CHO}]_3$  to the reaction mixture. The resulted gel was subjected to hydrothermal treatment in an autoclave at 423 K for 18–72 h. After then the solid was washed with distilled water until to get neutral pH and dried at room temperature.

### 2.3. Dye adsorption

Preliminary tests were performed to check the influence of pH on the dye adsorption process. Using the best pH conditions, the effect of contact time of dye with adsorbent was studied using dye concentration of  $3.50 \text{ mmol dm}^{-3}$ . Equilibrium studies were conducted using optimum value of contact time for all samples. Solutions of different concentrations ranging from 0.15 to  $3.50 \text{ mmol dm}^{-3}$  were used to construct the adsorption isotherms. To determine the amount of dye adsorbed on the fabricated silicate, dye-silicate dispersion was filtered and the concentration of dye was measured by UV-Vis absorption spectroscopy. From the isotherm experiments, the amount of dye adsorbed at equilibrium ( $q_e$ ) as mmol of adsorbate per gram of adsorbent ( $\text{mmol g}^{-1}$ ) was calculated using Eq. (1):

$$q_e = \frac{(C_0 - C_e)V}{m} \quad (1)$$

where  $C_0$  and  $C_e$  ( $\text{mmol dm}^{-3}$ ) are the initial and equilibrium liquid-phase concentrations of the adsorbate, respectively.  $V$  is the solution volume ( $\text{dm}^3$ ) and  $m$  is the adsorbent mass (g) [30]. In kinetic experiments, the amount of dye adsorbed at any time  $t$  ( $q_t$ ) in  $\text{mmol g}^{-1}$  was calculated with Eq. (2):

$$q_t = \frac{(C_0 - C_t)V}{m} \quad (2)$$

where  $C_t$  ( $\text{mmol dm}^{-3}$ ) is the dye concentration in the solution at any time  $t$  [30].

### 3. Characterization

Infrared (IR) spectra were taken with Equinox 55 (Bruker, Germany) spectrophotometer using a wavelength 4,000 to 400  $\text{cm}^{-1}$  and resolution of 4  $\text{cm}^{-1}$ . For sample preparation, 0.5% of the sample was pressed with KBr at a pressure of 7 ton  $\text{cm}^{-2}$ .

X-ray measurement was performed with XRD 7000 (Bruker) using a radiation source  $\text{CuK}\alpha$  ( $\lambda = 0.154$  nm) and scan rate of  $2.0^\circ 2\theta \text{ min}^{-1}$ .

Solid-state NMR spectra were recorded with 400 MHz Avance III (Bruker) spectrometer at room temperature. Samples were compacted into a zirconium rotor (diameter 7 mm) and measurements were taken at 59.61 MHz for  $^{29}\text{Si}$  and 104.27 MHz for  $^{27}\text{Al}$  nuclei using a magic angle spinning of 4 kHz.

Thermogravimetric analyses were performed with thermobalance 1090 B, using a heating rate of  $0.167 \text{ K s}^{-1}$ , under a nitrogen flow of  $30 \text{ cm}^3 \text{ s}^{-1}$ . Approximately 10 mg of the solid sample was analyzed at a temperature range from 298 to 1,273 K.

Nitrogen adsorption/desorption isotherms were measured with NOVA 4200 (Quantachrome, USA) at 77 K using a relative pressure ( $P/P^\circ$ ) from 0.05 to 0.30.

Scanning electron microscopy (SEM) images were taken with a JSM 6360-LV (Jeol, USA), operating at 20 kV.

The concentration of dye was measured at 417 nm on a spectrophotometer model MultiSpec TCC-1501-240A (Shimadzu) and pH of the solutions was measured with SevenEasy pH meter (Mettler Toledo, USA).

## 4. Results and discussion

### 4.1. Infrared spectroscopy

Infrared spectra of NaMG, [Al]NaMG and [2Al]NaMG silicates are shown in Fig. 2. The bands appeared in the range 3,640–3,590  $\text{cm}^{-1}$  and 1,660–1,628  $\text{cm}^{-1}$  represents stretching vibrations of O–H groups of water molecules trapped inside the silicate layers [12,31]. The band centered in the region 1,400–500  $\text{cm}^{-1}$  can be assigned to  $\text{SiO}_4$  framework, while the bands at 1,075  $\text{cm}^{-1}$  shows the asymmetric stretching and were assigned to Si–O–Si and Si–O– groups. The symmetric stretching vibrations of Si–O–Si were observed in the region 700–950  $\text{cm}^{-1}$  [32,33]. The same bands of the inorganic framework were maintained when Si were exchanged

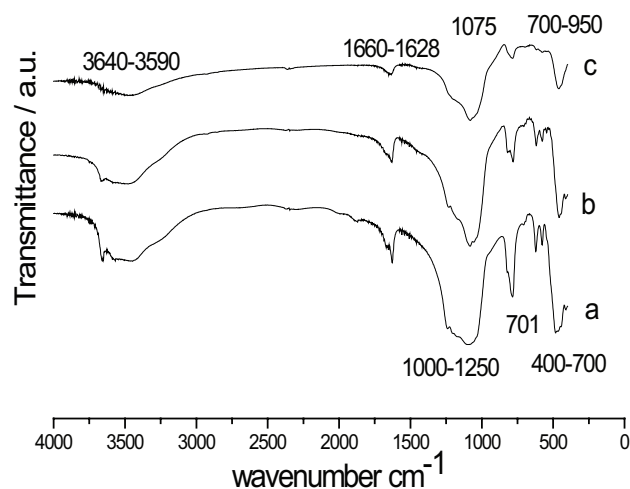


Fig. 2. IR spectra of (a) NaMG, (b) [Al]NaMG and (c) [2Al]NaMG.

by aluminum; however, the intensity of these peaks were decreased. Bands appeared in the 3,200–3,750  $\text{cm}^{-1}$  range can be assigned to silanol groups [34]. The band appeared at 701  $\text{cm}^{-1}$  in the spectrum of NaMG represents free silanol groups. A decrease in the intensity of this band was observed for aluminum modified silicates, which suggest the utilization of free silanol groups during the modification process [34].

### 4.2. NMR spectroscopy

The  $^{29}\text{Si}$  NMR spectrum of the original NaMG (Fig. 3(A)) gave signals at  $-110.6$  and  $-98.6$  ppm, and were assigned to  $\text{Q4}[\text{Si}(\text{OSi})_4]$  and  $\text{Q3}[\text{Si}(\text{OSi})_3(\text{O}-)]$  sites, respectively [35]. The insertion of Al in tetrahedral substitution in the silica framework modifies the chemical environment of the nearest silicon atoms, but also of their second and further neighbors. This leads to a modification of their chemical shifts. Shifting of the Q4 and Q3 signals can be clearly observed from Fig. 3. The increase in the Q3/Q4 ratio after modification is due to isomorphous substitution of Si by Al or possible formation of new silanol groups as previously reported [35,36].

The  $^{27}\text{Al}$  NMR spectra of the prepared materials (Fig. 3(B)) presented main signals at 63.2 ppm and were assigned to aluminum species in tetrahedral coordination [9,17]. The spectrum of [2Al]NaMG presented two main signals at 5.5 and 53.6 ppm, representing aluminum in octahedral and tetrahedral coordination [9,17].

### 4.3. X-ray diffraction

The XRD pattern (Fig. 4) of magadiites gave typical characteristic diffraction pattern at  $5.6^\circ$  (001);  $11.36^\circ$  (002);  $17.1^\circ$  (003);  $25.94^\circ$ ;  $25.92^\circ$ ;  $27.5^\circ$  and  $28.42^\circ$  corresponding to (hkl) lines with some cristobalite [9,17].

The modified samples [Al]NaMG and [2Al]NaMG gave the characteristic diffraction patterns of the parent material. The intensities of the diffraction peaks are similar to that of NaMG, however, for [2Al]NaMG broadening of diffraction peaks indicate lower degree of crystallization (associated with amorphous silica-alumina), or indicates that aluminum modified samples are mostly or completely amorphous [9,17].

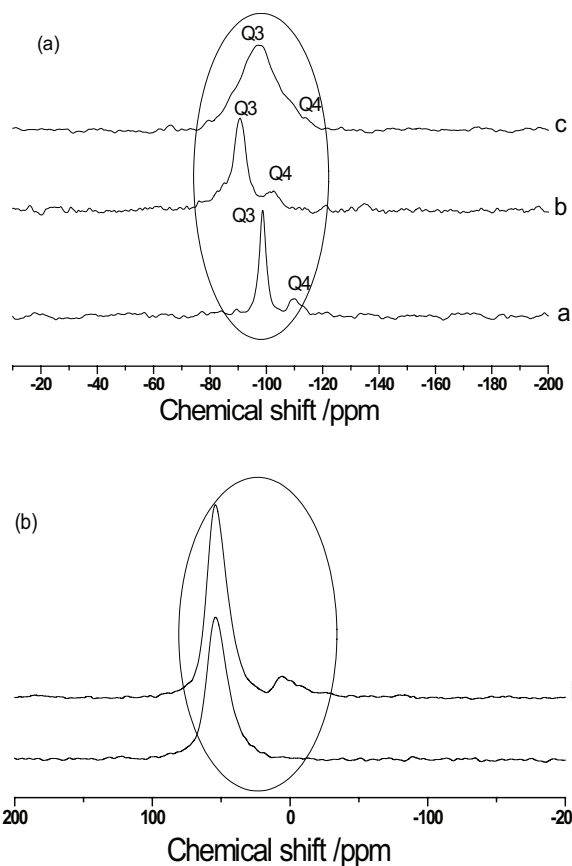


Fig. 3. (A)  $^{29}\text{Si}$  NMR CP-MAS spectra of (a) NaMG, (b) [Al]NaMG and (c) [2Al]NaMG and (B)  $^{27}\text{Al}$  NMR spectrum of (a) [Al]NaMG and (b) [2Al]NaMG.

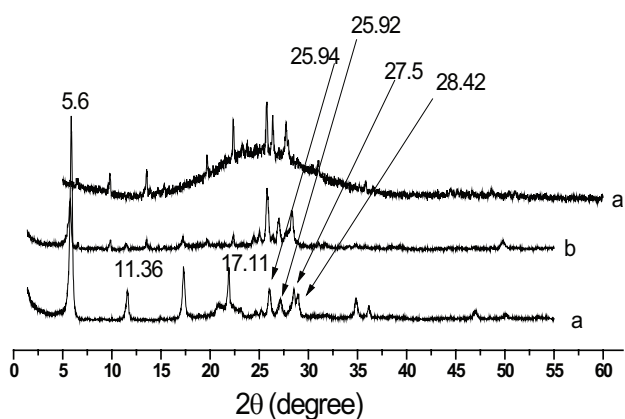


Fig. 4. XRD patterns of (a) NaMG, (b) [Al]NaMG and (c) 2[Al]NaMG.

#### 4.4. Scanning electron microscopy

SEM images of magadiite and aluminum modified silicates are shown in Figs. 5(A) and (B). Typical morphology of the magadiite was observed showing layered rosette-shaped morphology constructed by contact packing of well-defined plates [9,17,32].

The SEM images of [Al]NaMG (Figs. 5(C) and (D)) and [2Al]NaMG (Figs. 5(E) and (F)) indicates the existence of

the rosette as well as disk-shaped particles which confirm the existence of both crystalline and amorphous phases. The insertion of aluminum in silicate framework decreased the crystallinity and particle size of magadiite as observed also with XRD data [8,17,37], which resulted in an increase in surface area and dye adsorption capacity.

#### 4.5. Nitrogen adsorption/desorption

A summary of textural parameters obtained by  $\text{N}_2$  adsorption/desorption is given in Table 1. The BET surface area of the magadiite was observed to be  $27 \text{ m}^2 \text{ g}^{-1}$ . An increment in the surface area was observed after the insertion of aluminum in silicate framework. For [Al]NaMG and [2Al]NaMG materials the surface area increased from 27 to  $104 \text{ m}^2 \text{ g}^{-1}$  and  $140 \text{ m}^2 \text{ g}^{-1}$ , respectively, which can be tentatively assigned to the presence of the disk-shaped particles and decrease in particle size as observed by SEM images.

#### 4.6. Thermogravimetry

Thermogravimetry (TG) and its derivative (DTG) curves for NaMG, [Al]NaMG and [2Al]NaMG are shown in Figs. 6(A) and (B). Irrespective of the cristobalite contents, the curves for these synthesized silicates are very similar, varying with regard to the physisorbed water. The synthesized silicates presented three mass losses at 350, 394 and 567 K for NaMG, at 357, 403 and 562 K for [Al]NaMG and at 337, 367 and 629 K for [2Al]NaMG. These events can be assigned to the elimination of water molecules during the heating process, either bonded through hydrogen bonding or bonded to the adsorbent surface [8,22,31,38].

#### 4.7. Dye removal

The dye adsorption process strongly depends on adsorbent and adsorbate structure and dissociation of adsorbate to produce neutral, positive or negative charges. Preliminary tests were performed to check the influence of pH and contact time on the adsorption process. For this purpose solution of different concentrations ranging from  $0.15$  to  $3.5 \text{ mmol dm}^{-3}$  were prepared.

#### 4.8. Effect of pH

Variation in dye uptake at different pH values was investigated by taking about 20 mg of each material dispersed in dye solution ( $10.0 \text{ cm}^3$  of  $3.0 \text{ mmol dm}^{-3}$ ) at  $298 \pm 1 \text{ K}$ . After 8 h, the solutions (of varying pH) were analyzed spectrophotometrically at a wavelength of 620 nm. Dye removal was maximum at low pH (3–6) while minimum dye was removed at high pH (7–9), when the pH was increased to 9, a decrease in dye adsorption was observed (Fig. 7). For aluminum incorporated silicates, increase in dye uptake was observed when compared with unmodified material, which is probably due to the presence of Al basic sites which can attract the negatively charged dye molecules [39]. Thus, acidic or basic pH interferes in the adsorption process depending on the system characteristics (adsorbent and adsorbate).

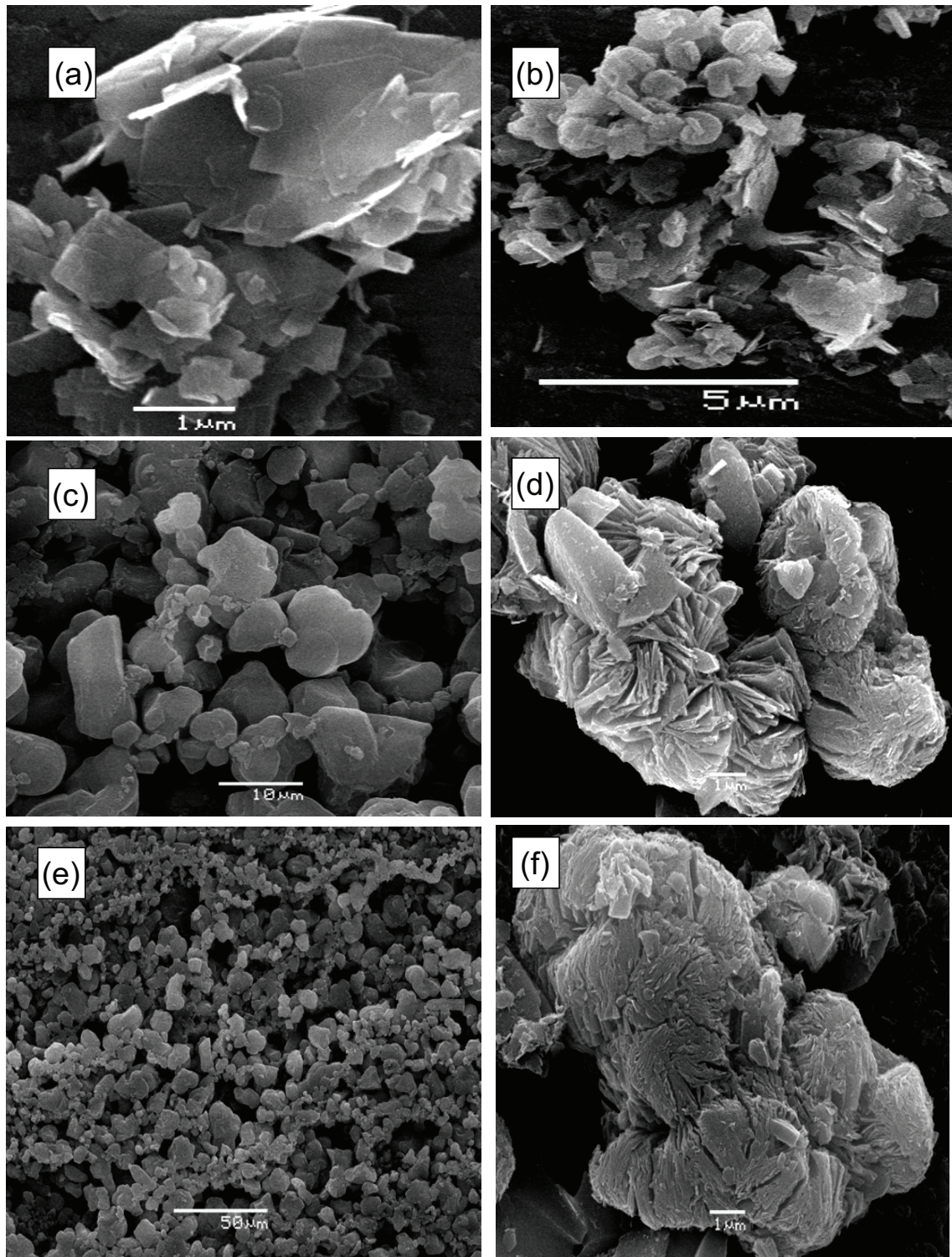


Fig. 5. (A) and (B) SEM images of NaMG, (C) and (D) [Al]NaMG, and (E) and (F) [2Al]NaMG.

#### 4.9. Kinetic studies

The dye adsorption efficiency of the synthesized silicates was determined by considering the influence of contact time with dye molecules. This process is regarded as a reversible reaction at the solid/liquid interface. Adsorption kinetic

studies were performed by taking about 20 mg of each material dispersed in 10.0 cm<sup>3</sup> of RY solutions (3.0 mmol dm<sup>-3</sup>) at 298 ± 1 K. At regular time intervals aliquots of the supernatant were analyzed spectrophotometrically at correspondent  $\lambda_{\max}$ . The resultant kinetic isotherms are shown in Fig. 8.

Table 1  
Surface area obtained with the BET method ( $S_{\text{BET}}$ ) and Si/Al ratio

Materials	$S_{\text{BET}}/\text{m}^2 \text{g}^{-1}$	Si/Al
NaMG	27	nil
[Al]NaMG	104	82
[2Al]NaMG	140	41

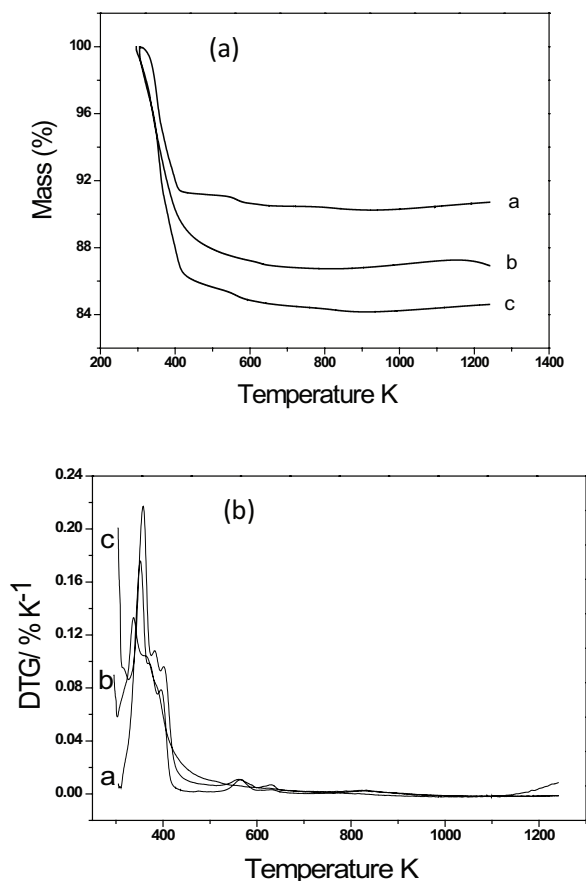


Fig. 6. (A) TG curves of (a) NaMG, (b) [Al]NaMG and (c) [2Al]NaMG, and (B) DTG curves of (a) NaMG, (b) [Al]NaMG and (c) [2Al]NaMG.

The dye uptake increased with time and reached a constant value, represented by the constancy, as shown in Fig. 8. The equilibrium states were attained within 150, 180 and 200 min for NaMG, [Al]NaMG and [2Al]NaMG, respectively. No significant difference in adsorption was observed when the contact time was longer than this value.

The pseudo-first-order and pseudo-second-order kinetic models [40,41] were applied to study the adsorption kinetic behavior and the obtained data were processed to understand the dynamics of RY adsorption onto silicates in terms of order and rate constants. The differential equation for the pseudo-first-order kinetic model is given by Eq. (3) and the pseudo-second-order kinetic model is given in Eq. (4):

$$\frac{dq_t}{dt} = k_1(q_e - q_t) \quad (3)$$

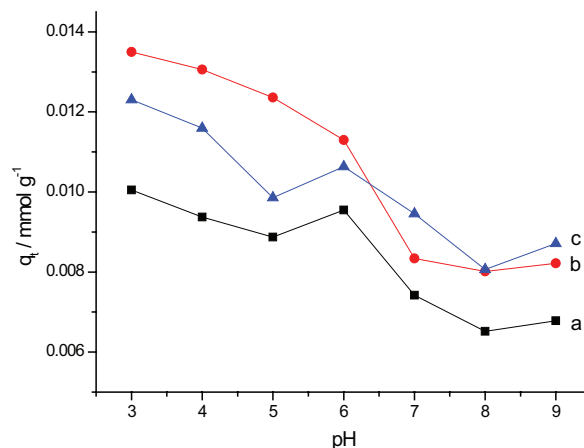


Fig. 7. Effect of pH on adsorption capacity of materials (a) NaMG, (b) [Al]NaMG and (c) [2Al]NaMG for remazol yellow.

$$\frac{dq_t}{dt} = k_2(q_e - q_t)^2 \quad (4)$$

where  $q_e$  and  $q_t$  refer to the amounts of dye adsorbed ( $\text{mg g}^{-1}$ ) at equilibrium and at any time,  $t$  (min), respectively, and  $k_1$  is the equilibrium rate constant of pseudo-first-order adsorption ( $\text{min}^{-1}$ ) and  $k_2$  ( $\text{g mg}^{-1} \text{min}^{-1}$ ) is the rate constant of pseudo-second-order adsorption.

The correlation coefficients ( $R^2$ ) of the non-linear fit of pseudo-first-order and pseudo-second-order for the adsorption of RY onto NaMG, [Al]NaMG and [2Al]NaMG are listed in Table 2. The rate constant,  $k_1$  and equilibrium adsorption capacity ( $q_e$ ) were calculated from the plots of  $\log(q_e - q_t)$  vs.  $t$ . The high  $R^2$  values were obtained with pseudo-first-order kinetics and indicate that the adsorption of RY onto magadiites is an ideal pseudo-first-order reaction. The rate constant  $k_1$  values were found to be 0.039, 0.033 and 0.026  $\text{min}^{-1}$  for NaMG, [Al]NaMG and [2Al]NaMG, respectively. The calculated  $q_e$  values with pseudo-first-order are also very close to the experimental values ( $q_{\text{exp}}$ ) (Table 2), indicating that the adsorption of RY onto these magadiites follows the proposed kinetic model. The lower chi-square value ( $\chi^2$ ) indicates a good fit of the model to the experimental data.

#### 4.10. Adsorption isotherms

The amount of RY dye adsorbed on magadiites as a function of concentration is shown in Fig. 9. The obtained data from the adsorption isotherms were used to calculate the adsorption capacity  $q_e$  ( $\text{mmol g}^{-1}$ ) of the adsorbents by a mass balance relationship [42]. The fabricated samples presented a very similar behavior representing a possible multilayer adsorption process or the presence of two distinct adsorption sites. The insertion of aluminum favors the adsorption process as previously reported [21,43,44].

A comparison of the maximum adsorption capacities for a series of synthesized materials is given in Table 3. When compared with modified nanocellulose [44], Fe-zeolitic tuff [45] and modified silicas [21,43,46] materials, despite of very low surface area (NaMG:  $27 \text{ m}^2 \text{g}^{-1}$ , [Al]NaMG:  $104 \text{ m}^2 \text{g}^{-1}$  and [2Al]NaMG:  $140 \text{ m}^2 \text{g}^{-1}$ ) our synthesized materials showed

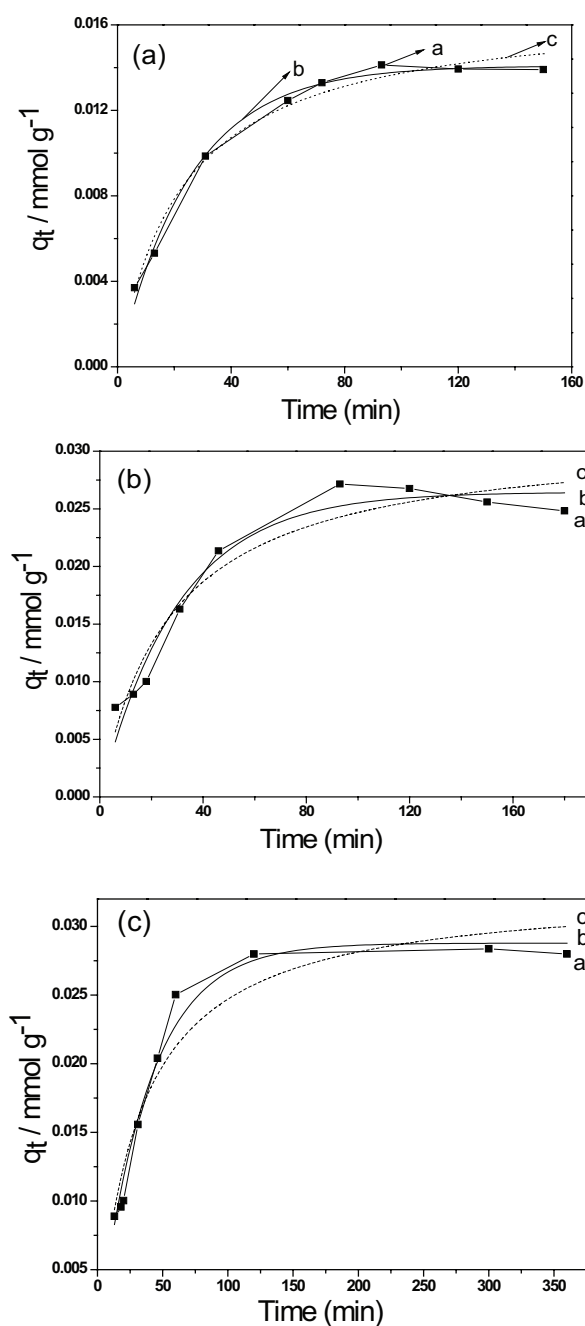


Fig. 8. Adsorption kinetic isotherms of RY dye onto magadiites (A) NaMG, (B) [Al]NaMG and (C) [2Al]NaMG: (a) experimental and with adjustment to the (b) pseudo-first-order and (c) pseudo-second-order models at  $298 \pm 1$  K.

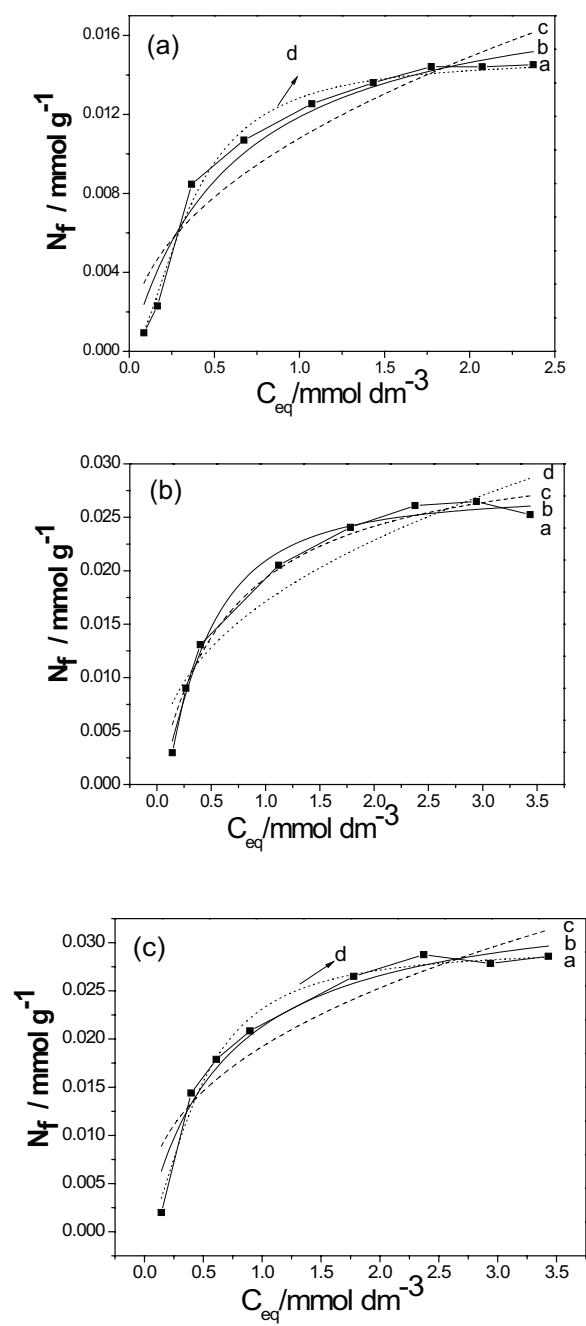


Fig. 9. Sorption isotherms for RY dye onto magadiites (A) NaMG, (B) [Al]NaMG and (C) [2Al]NaMG: (a) experimental and with adjustment to the (b) Langmuir, (c) Freundlich and (d) Sips models at  $298 \pm 1$  K.

Table 2  
Comparison of the pseudo-first-order and pseudo-second-order kinetic models for remazol yellow

Material	Exp $q_{exp}$ (mmol g <sup>-1</sup> )	Pseudo-first-order				Pseudo-second-order			
		$q_e$ (mmol g <sup>-1</sup> )	$k_1$ (min <sup>-1</sup> )	$R^2$	$\chi^2 \times 10^{-7}$	$q_e$ (mmol g <sup>-1</sup> )	$k_2$ (min <sup>-1</sup> )	$R^2$	$\chi^2 \times 10^{-7}$
NaMG	0.014	$0.014 \pm 0.000$	$0.039 \pm 0.002$	0.99	1.53	$0.017 \pm 0.001$	$2.570 \pm 0.430$	0.98	3.198
[Al]NaMG	0.026	$0.026 \pm 0.001$	$0.033 \pm 0.004$	0.95	29.59	$0.031 \pm 0.002$	$1.164 \pm 0.333$	0.93	44.97
[2Al]NaMG	0.028	$0.029 \pm 0.001$	$0.026 \pm 0.002$	0.98	15.73	$0.032 \pm 0.002$	$0.945 \pm 0.234$	0.93	53.03

good adsorption capacities. Taking into account the obtained results, it could be concluded that increase in aluminum content in the silicate structure favors the adsorption process [21].

Adsorption isotherms demonstrate how the adsorbate molecules can be distributed between solid/liquid interfaces at equilibrium. To get insight into the adsorption mechanism, surface properties and affinity of the adsorbent, the Langmuir [47], Freundlich [48] and Sips isotherm models [49] were assayed (Eqs. (5)–(7)) and the obtained results are given in Table 4.

$$N_f = \frac{N_{\text{mon}} b_L C_{\text{eq}}}{1 + b_L C_{\text{eq}}} \quad (5)$$

$$N_f = K_f (C_{\text{eq}})^{1/n} \quad (6)$$

$$N_f = \frac{N_{\text{mon}} b_s (C_{\text{eq}})^{1/n}}{1 + b_s (C_{\text{eq}})^{1/n}} \quad (7)$$

where  $N_f$  (mmol g<sup>-1</sup>) is equivalent to  $q_e$ ,  $C_{\text{eq}}$  is the concentration of dye present at equilibrium,  $N_{\text{mon}}$  is the maximum

Table 3

Comparison of adsorption capacity ( $Q_m$ ) of different materials for remazol yellow dye (RY GR)

Sorbent	Dye	$Q_m$ /mmol g <sup>-1</sup>	Reference
Fe-zeolitic tuff	RY GR	0.004	[45]
NaMG	RY GR	0.014	This work
Modified nanocellulose	RY GR	0.026	[44]
[Al]NaMG	RY GR	0.026	This work
[2Al]NaMG	RY GR	0.028	This work
Mesoporous aminopropyl silica	RY GR	0.037	[46]
Si-APMP	RY GR	0.553	[43]
SBA-15	RY GR	0.725	[21]
[Al]SBA-15	RY GR	0.791	[21]
[2Al]SBA-15	RY GR	0.821	[21]

Table 4

Adsorption results of RY dye on silicates, using several adsorption models, to give the coefficient of correlation ( $R^2$ ), Langmuir constants ( $b_L$ ), Freundlich constant ( $K_f$ ), Sips heterogeneity factor ( $n_s$ ), Sips constant ( $b_s$ ) experimental ( $q_{\text{exp}}$ ) and theoretical ( $N_f$ ) adsorption capacities

Material	Exp $q_{\text{exp}}$ (mmol g <sup>-1</sup> )	Langmuir			Freundlich			Sips			
		$R^2$	$N_f$ (mmol g <sup>-1</sup> )	$K_L$	$R^2$	$N_f$ (mmol g <sup>-1</sup> )	$n$	$R^2$	$N_f$ (mmol g <sup>-1</sup> )	$b_s$	$n_s$
NaMG	0.014	0.96	0.019 ± 0.002	1.6	0.88	0.011 ± 0.001	2.1	0.99	0.015 ± 0.001	6.3 ± 2.1	0.55
[Al]NaMG	0.026	0.97	0.032 ± 0.001	1.5	0.90	0.017 ± 0.001	2.3	0.99	0.027 ± 0.001	3.3 ± 1.09	0.67
[2Al]NaMG	0.028	0.95	0.035 ± 0.002	1.5	0.85	0.019 ± 0.001	2.5	0.98	0.029 ± 0.001	3.7 ± 1.08	0.59

quantity of adsorbate required for monolayer formation,  $b_L$  is the affinity of the binding sites and energy of adsorption that includes the equilibrium constant for Langmuir. The values  $K_f$  and  $n$  are the Freundlich constants related to the extent of adsorption and the degree of nonlinearity between solution concentration and adsorption, respectively,  $b_s$  is the Sips constant that is related to the adsorption energy or adsorption affinity and resembles the  $b_L$  parameter of the Langmuir model. Parameter  $n_s$  is the Sips constant related to the surface heterogeneity.

The constants for these adsorption models and the linear regression correlations ( $R^2$ ) for the isotherms are listed in Table 4. The adsorption data were poorly fitted to the Langmuir and Freundlich models, as evidenced from lower  $R^2$  values. The Sips model resulted in high  $R^2$  and best explains the adsorption mechanism. The constant  $b_s$  values ≤ 10 indicated that the adsorption of RY on Al-magadiites is a favorable process [44,50]. The equilibrium curves along with fitted models are shown in Fig. 9. The maximum adsorption capacities ( $N_f$ ) of NaMG, [Al]NaMG and [2Al]NaMG obtained with Sips model are in agreement with the experimental values.

The Sips heterogeneity factor  $n_s$  is used to predict the adsorption on heterogeneous system and thus plays a major role in determining the interaction types between the dye and magadiite surface. It is related to the existence of lateral interactions between the adsorbed molecules, which is not considered in the Langmuir theory. Thus the obtained  $n_s$  values ≤ 1 for NaMG, [Al]NaMG and [2Al]NaMG (Table 4) suggest that these silicates have heterogeneous surfaces with adsorption sites and have different adsorption energies and also confirm the multilayer coverage of RY on the silicate surface. All isotherm model parameters were performed using OriginPro 8 software.

## 5. Conclusion

The precursor lamellar silicate has a stable structure. The insertion of aluminum in the silicate structure not only increased the surface area but also created Lewis acidic centers which can interact more strongly with negatively charged dye molecules

Batch wise adsorption studies showed the effectiveness of these synthesized materials as efficient adsorbents for reactive dye remazol yellow, considering the best experimental conditions to reach the equilibrium in aqueous

solution. Kinetic models showed good agreement between the experimental and expected values. The Sips isotherm was found to provide a close fit to the equilibrium data. The aluminum modified silicates have the ability to remove RY dye from water.

This investigation also provides an evidence of bonding interactions of RY dye with the Al incorporated silicates surface. These synthesized materials can be recommended as convenient and useful materials to remove reactive dyes such as remazol yellow from water.

### Acknowledgment

The authors acknowledge TWAS/CNPq (Grant No. 190156/2010-4) for fellowships and financial support.

### References

- [1] M. Yang, A current global view of environmental and occupational cancers, *J. Environ. Sci. Health C Environ. Carcinog. Ecotoxicol. Rev.*, 29 (2011) 223–49.
- [2] L. Cirera, M. Rodríguez, J. Giménez, E. Jiménez, M. Saez, J.-J. Guillén, J. Medrano, M.-A. Martínez-Victoria, F. Ballester, S. Moreno-Grau, C. Navarro, Effects of public health interventions on industrial emissions and ambient air in Cartagena, Spain, *Environ. Sci. Pollut. Res. Int.*, 16 (2009) 152–161.
- [3] E.M. Öncü-Kaya, N. Şide, Ö. Gök, A.S. Özcan, A. Özcan, Evaluation on dye removal capability of didodecyldimethylammonium-bentonite from aqueous solutions, *J. Dispersion Sci. Technol.*, 38 (2017) 1211–1220.
- [4] A.E. Segneanu, C. Orbeci, C. Lazau, P. Sfirloaga, P. Vlazan, C. Bantas, I. Grozescu, Waste Water Treatment Methods, in: *Water Treatment*, 2013, pp. 53–80.
- [5] L. Lu, J. Li, J. Yu, P. Song, D.H.L. Ng, A hierarchically porous  $MgFe_2O_4/\gamma-Fe_2O_3$  magnetic microspheres for efficient removals of dye and pharmaceutical from water, *Chem. Eng. J.*, 283 (2016) 524–534.
- [6] J.E. Aguiar, J.A. Cecilia, P.A.S. Tavares, D.C.S. Azevedo, E. Rodriguez Castellón, S.M.P. Lucena, I.J. Silva, Adsorption study of reactive dyes onto porous clay heterostructures, *Appl. Clay Sci.*, 135 (2017) 35–44.
- [7] A.S.O. Moscofian, C.T. Pires, A.P. Vieira, C. Airoidi, Organofunctionalized magnesium phyllosilicates as mono-or bifunctional entities for industrial dyes removal, *RSC Adv.*, 2 (2012) 3502–3511.
- [8] C.T.G.V.M.T. Pires, J.R. Costa, C. Airoidi, Isomorphous silicon/aluminum substitution on layered ilerite – structural study and calorimetry of copper interaction, *Microporous Mesoporous Mater.*, 163 (2012) 1–10.
- [9] C.T.G.V.M.T. Pires, N.G. Oliveira, C. Airoidi, Structural incorporation of titanium and/or aluminum in layered silicate magadiite through direct syntheses, *Mater. Chem. Phys.*, 135 (2012) 870–879.
- [10] T.R. Macedo, G.C. Petrucelli, C. Airoidi, Silicic acid magadiite as a host for n-alkyldiamine guest molecules and features related to the thermodynamics of intercalation, *Clays Clays Miner.*, 9 (2007) 151–159.
- [11] A. Gil, S.A. Korili, R. Trujillano, M.A. Vicente, A review on characterization of pillared clays by specific techniques, *Appl. Clay Sci.*, 53 (2011) 97–105.
- [12] B. Royer, N.F. Cardoso, E.C. Lima, T.R. Macedo, C. Airoidi, Sodic and acidic crystalline lamellar magadiite adsorbents for the removal of methylene blue from aqueous solutions: kinetic and equilibrium studies, *Sep. Sci. Technol.*, 45 (2009) 129–141.
- [13] Z. Wu, D. Zhao, Ordered mesoporous materials as adsorbents, *Chem. Commun.*, 47 (2011) 3332–3338.
- [14] T. Selvam, C. Aresipathi, G.T.P. Mabande, H. Toufar, W. Schwieger, Solid state transformation of TEAOH-intercalated kanemite into zeolite beta (BEA), *J. Mater. Chem.*, 15 (2005) 2013–2019.
- [15] A. Corma, F. Rey, S. Valencia, J.L. Jorda, J. Rius, A zeolite with interconnected 8-, 10- and 12-ring pores and its unique catalytic selectivity, *Nat. Mater.*, 2 (2003) 493–497.
- [16] H.M. Moura, H.O. Pastore, Functionalized mesoporous solids based on magadiite and [Al]-magadiite, *Dalton Trans.*, 43 (2014) 10471–10483.
- [17] Y. Bi, J. Blanchard, J.-F. Lambert, Y. Millot, S. Casale, S. Zeng, H. Nie, D. Li, Role of the Al source in the synthesis of aluminum magadiite, *Appl. Clay Sci.*, 57 (2012) 71–78.
- [18] E.M. Barea, V. Fornes, A. Corma, P. Bourges, E. Guillon, V.F. Puentes, A new synthetic route to produce metal zeolites with subnanometric magnetic clusters, *Chem. Commun.*, 17 (2004) 1974–1975.
- [19] W. Supronowicz, Influence of Presence of a Heteroatom Source on the Synthesis of Layered Silicates-Ilerite, Magadiite and Kenyaite (Doctoral dissertation, Universität Oldenburg), 2011.
- [20] G. Lagaly, K. Beneke, Magadiite and H-magadiite: I. Sodium Magadiite and Some of Its Derivatives, *Am. Mineral.*, 60 (1975) 642–649.
- [21] K. Ahmed, F. Rehman, C.T.G.V.M.T. Pires, A. Rahim, A.L. Santos, C. Airoidi, Aluminum doped mesoporous silica SBA-15 for the removal of remazol yellow dye from water, *Microporous Mesoporous Mater.*, 236 (2016) 167–175.
- [22] F. Kooli, L. Mianhui, S.F. Alshahateet, F. Chen, Z. Yinghuai, Characterization and thermal stability properties of intercalated Na-magadiite with cetyltrimethylammonium (C16TMA) surfactants, *J. Phys. Chem. Solids*, 67 (2006) 926–931.
- [23] W. Schwieger, G. Lagaly, Alkali Silicates and Crystalline Silicic Acids. Handbook of Layered Materials, Marcel Dekker, Inc., New York, Basel, 2004.
- [24] S. Li, Y. Mao, H.J. Ploehn, Mechanical reinforcement in magadiite/styrene-butadiene rubber composites, *J. Appl. Polym. Sci.*, 134 (2017) 44763.
- [25] E.M. Usai, M.F. Sini, D. Meloni, V. Solinas, A. Salis, Sulfonic acid-functionalized mesoporous silicas: microcalorimetric characterization and catalytic performance toward biodiesel synthesis, *Microporous Mesoporous Mater.*, 179 (2013) 54–62.
- [26] S.J. Kim, M.H. Kim, G. Seo, Y.S. Uh, Preparation of tantalum-pillared magadiite and its catalytic performance in Beckmann rearrangement, *Res. Chem. Intermed.*, 38 (2012) 1181–1190.
- [27] X. Sun, J. King, J.L. Anthony, Molecular sieve synthesis in the presence of tetraalkylammonium and dialkylimidazolium molten salts, *Chem. Eng. J.*, 147 (2009) 2–5.
- [28] Y. Chen, G. Yu, F. Li, J. Wei, Structure and photoluminescence of composite based on ZnO particles inserted in layered magadiite, *Appl. Clay Sci.*, 88 (2014) 163–169.
- [29] S. Wang, H. Li, S. Xie, S. Liu, L. Xu, Physical and chemical regeneration of zeolitic adsorbents for dye removal in wastewater treatment, *Chemosphere*, 65 (2006) 82–87.
- [30] W.-T. Tsai, K.-J. Hsien, H.-C. Hsu, Adsorption of organic compounds from aqueous solution onto the synthesized zeolite, *J. Hazard. Mater.*, 166 (2009) 635–641.
- [31] C. Eypert-Blaison, E. Sauzéat, M. Pelletier, L.J. Michot, F. Villiéras, B. Humbert, Hydration mechanisms and swelling behavior of Na-magadiite, *Chem. Mater.*, 13 (2001) 1480–1486.
- [32] G.B. Superti, E.C. Oliveira, H.O. Pastore, A. Bordo, C. Bisio, L. Marchese, Aluminum magadiite: an acid solid layered material, *Chem. Mater.*, 19 (2007) 4300–4315.
- [33] A.G.S. Prado, J.A.A. Sales, R.M. Carvalho, J.C. Rubim, C. Airoidi, Immobilization of 5-amino-1,3,4-thiadiazole-thiol onto silica gel surface by heterogeneous and homogeneous routes, *J. Non-Cryst. Solids*, 333 (2004) 61–67.
- [34] F. Rehman, P.L.O. Volpe, C. Airoidi, The applicability of ordered mesoporous SBA-15 and its hydrophobic glutaraldehyde-bridge derivative to improve ibuprofen-loading in releasing system, *Colloids Surf., B*, 119 (2014) 82–89.
- [35] J.S. Dailey, T.J. Pinnavaia, Silica-pillared derivatives of H<sup>+</sup>-magadiite, a crystalline hydrated silica, *Chem. Mater.*, 4 (1992) 855–863.
- [36] S.-T. Wong, S. Cheng, Preparation and characterization of pillared magadiite, *Chem. Mater.*, 6 (1993) 770–777.
- [37] P. Heinrich Thiesen, K. Beneke, G. Lagaly, Silylation of a crystalline silicic acid: an MAS NMR and porosity study, *J. Mater. Chem.*, 12 (2002) 3010–3015.

- [38] F. Kooli, L. Yan, Thermal stable cetyltrimethylammonium-magadiites: influence of the surfactant solution type, *J. Phys. Chem. C*, 113 (2009) 1947–1952.
- [39] B. Dragoi, E. Dumitriu, C. Guimon, A. Auroux, Acidic and adsorptive properties of SBA-15 modified by aluminum incorporation, *Microporous Mesoporous Mater.*, 121 (2009) 7–17.
- [40] H. Arslanoglu, H.S. Altundogan, F. Tumen, Heavy metals binding properties of esterified lemon, *J. Hazard. Mater.*, 164 (2009) 1406–1413.
- [41] Y.S. Ho, G. McKay, Pseudo-second order model for sorption processes, *Process Biochem.*, 34 (1999) 451–465.
- [42] G. Engelhardt, D. Michel, *High-Resolution Solid-State NMR of Silicates and Zeolites*, John Wiley and Sons, Australia, 1987.
- [43] A.S.O. Moscofian, C.T. Pires, A.P. Vieira, C. Airoidi, Removal of reactive dyes using organofunctionalized mesoporous silicas, *J. Porous Mater.*, 20 (2013) 1179–1188.
- [44] K. Xie, W. Zhao, X. He, Adsorption properties of nano-cellulose hybrid containing polyhedral oligomeric silsesquioxane and removal of reactive dyes from aqueous solution, *Carbohydr. Polym.*, 83 (2011) 1516–1520.
- [45] M.J. Solache-Rios, R. Villalva-Coyote, M. del C. Díaz-Nava, Sorption and desorption of remazol yellow by a Fe-zeolitic tuff, *J. Mex. Chem. Soc.*, 54 (2010) 59–68.
- [46] A.R. Cestari, E.F.S. Vieira, G.S. Vieira, L.E. Almeida, Aggregation and adsorption of reactive dyes in the presence of an anionic surfactant on mesoporous aminopropyl silica, *J. Colloid Interface Sci.*, 309 (2007) 402–411.
- [47] I. Langmuir, Adsorption of gases on plain surfaces of glass mica platinum, *J. Am. Chem. Soc.*, 40 (1918) 1361–1403.
- [48] H. Freundlich, W. Heller, The adsorption of cis- and trans-azobenzene, *J. Am. Chem. Soc.*, 61 (1939) 2228–2230.
- [49] M.C. Carter, J.E. Kilduff, W.J. Weber, Site energy distribution analysis of preloaded adsorbents, *Environ. Sci. Technol.*, 29 (1995) 1773–1780.
- [50] G.J.D.A.A. Soler-Illia, C. Sanchez, B. Lebeau, J. Patarin, Chemical strategies to design textured materials: from microporous and mesoporous oxides to nanonetworks and hierarchical structures, *Chem. Rev.*, 102 (2002) 4093–4138.